Monitoring statistics of the ERS-2 scatterometer for ESA

Cycle 139

Hans Hersbach

European Centre for Medium-Range Weather Forecasts,
Shinfield Park, Reading, RG2 9AX, England
Tel: (+44 118) 9499476, e-mail: dal@ecmwf.int

September 17, 2008

1   Introduction

The quality of the UWI product was monitored at ECMWF for Cycle 139. Results were compared to those obtained from the previous Cycle, as well for data received during the nominal period in 2000 (up to Cycle 59). No corrections for duplicate observations from overlapping ground stations were applied.

During Cycle 139 data was received between 21:06 UTC 4 August 2008 and 19:47 UTC 8 September 2008. Data was grouped into 6-hourly batches (centred around 00, 06, 12 and 18 UTC). No data was received in the batches for 00 UTC and 06 UTC 20 August 2008, and for 06 UTC 1 September 2008.

Data is being recorded whenever within the visibility range of a ground station. For Cycle 139, data coverage was over the North-Atlantic, part of the Mediterranean, the Gulf of Mexico, a small part of the Pacific west from the US, Canada and Central America, a small part of the Atlantic and Indian Ocean around South Africa, the Chinese Sea, a small part of the Indian Ocean south-east of Thailand and Indonesia, and the Southern Ocean close to the Antarctic and south of Australia and New Zealand (see Figure 2).

The asymmetry between the fore and aft incidence angles did not show large peaks. There was hardly any solar activity during Cycle 139 (source www.spaceweather.com).

Compared to Cycle 138, the UWI wind speed relative to ECMWF first-guess (FG) fields showed a similar standard deviation (1.31 m/s, was 1.29 m/s). Bias levels were somewhat less negative (on average -1.04 m/s, was -1.11 m/s).

Ocean calibration shows that inter-node and inter-beam dependencies of bias levels continues to be large. Average bias levels were less negative (-0.90 dB, was -0.97 dB; see

Figure 4).

The ECMWF operational assimilation and forecast system was not changed during Cycle 139.

The Cycle-averaged evolution of performance relative to ECMWF first-guess (FG) winds is displayed in Figure 1. Figure 2 shows global maps of the over Cycle 139 averaged UWI data coverage and wind climate, Figure 3 for performance relative to FG winds.

2 ERS-2 statistics from 4 August 2008 to 8 September 2008

2.1 Sigma0 bias levels

The average sigma0 bias levels (compared to simulated sigma0's based on ECMWF model FG winds) stratified with respect to antenna beam, ascending or descending track and as function of incidence angle (i.e. across-node number) is displayed in Figure 4.

Compared to Cycle 138, inter-node and inter-beam dependencies between the fore and aft antenna are similarly large. For the ascending tracks, the gap between the fore/aft and mid beam is considerable. Average bias level became 0.07 dB less negative (-0.90 dB), was -0.97 dB), being around 0.5 dB more negative than for nominal data in 2000 (around -0.4 dB; see Figure 1 of the reports for Cycle 48 to 59). The negative level in bias is not uncommon for the time of this year. The current situation is similar to that of one year ago (see e.g. the report for Cycle 127).

Long-term variations correlate with the yearly cycle, which, given the non-global coverage, is understandable. Therefore, the method of ocean calibration will probably only provide accurate information on calibration levels for globally or yearly averaged data sets.

The data volume of descending tracks was about 1% higher than for ascending tracks.

2.2 Incidence angles

For ESACA, across-node binning is, like the old processor, retained on a 25km mesh. From simple geometrical arguments it follows that variations in yaw attitude will lead to asymmetries between the incidence angles of the fore and aft beam. Indeed, this has been observed. Figure 5 gives a time evolution of this asymmetry. Also in this Figure, the occasions for which the combined k_p-yaw quality flag was set are indicated by red stars. The relation with incidence-angle asymmetries is obvious.

No large peaks occurred during Cycle 139. Solar activity was very low, although some gusts in the solar wind hit the Earth around 18 August 2008 and 6 September 2008 (source: www.spaceweather.com). These events did not have a noticeable effect on the ERS-2 yaw attitude.

2.3 Distance to cone history

The distance to the cone history is shown in Figure 6. Curves are based on data that passed all QC, including the test on the k_p-yaw flag, and subject to the land and sea-ice check at ECMWF (see cyclic report 88 for details).

Like for previous Cycles, time series are (due to lack of statistics) very noisy, especially for the near-range nodes. Most spikes were found to be the result of low data volumes.

Compared to Cycle 138, the average level was stable (1.20 versus 1.21), which is higher (by 10%) than for nominal data (see top panel Figure 1).

The fraction of data that did not pass QC is displayed in Figure 6 as well (dashed curves).

2.4 UWI minus First-Guess wind history

In Figure 7, the UWI minus ECMWF first-guess wind-speed history is plotted.

The history plot shows a few peaks, which are usually the result of low data volume.

Figure 11 displays the locations for which UWI winds were more than 8 m/s weaker (top panel), respectively more than 8 m/s stronger (lower panel) than FG winds. Like for Cycle 138, such collocations are isolated, and often indicate meteorologicaly active regions, for which UWI data and ECMWF model field show reasonably small differences in phase and/or intensity. Deviations near the poles are the result of imperfect sea-ice flagging.

One case for which UWI winds were considerably different from FG winds is presented in Figure 12. It concern the capture of hurricane Hanna (being at tropical-storm strength at that point) around Cuba on 3 September 2008. Besides that UWI winds are lower than the ECMWF FG, there is a de-aliasing problem in the south-western part of the swath (top panel of Figure 12). Both issues were addressed in the usage of these scatterometer data in the ECMWF analysis system, where the wind product is based on CMOD5.4 (stronger winds), and de-aliasing is performed dynamically. This is illustrated in the lower panel of Figure 12. Large, solid barbs indicate actively and selected wind solutions, while small, light barbs represent data that were not used (mainly because of a thinning to 100km). The effect of the ERS-2 scatterometer winds on the ECMWF analysis was a small displacement of the cyclone vortex to the west (dark/grey lines indicate surface-wind streamlines for the ECMWF analysis/first guess). Note that the small patch west of Cuba, with winds more or less perpendicular to the ECMWF fields, could not be well addressed. Given its oddness compared to surrounding winds in the ERS-2 swath, winds in this patch are likely anomalous.

Average bias levels and standard deviations of UWI winds relative to FG winds are displayed in Table 1. From this it follows that the bias of UWI winds was less negative (-1.04 m/s, was -1.11 m/s), being around -0.2 m/s more negative than for nominal data in 2000.

On a longer time scale seasonal bias trends are observed (see Figure 1). As was highlighted in previous cyclic reports, it is believed that this yearly trend is partly induced by changing local geophysical conditions. Strong indication for this is a similar trend

	Cycle 138		Cycle 139	
	UWI	CMOD4	UWI	CMOD4
speed STDV	1.29	1.29	1.31	1.30
node 1-2	1.34	1.33	1.38	1.36
node 3-4	1.29	1.28	1.33	1.32
node 5-7	1.25	1.25	1.28	1.28
node 8-10	1.24	1.24	1.25	1.25
node 11-14	1.27	1.27	1.26	1.25
node 15-19	1.27	1.28	1.27	1.27
speed BIAS	-1.11	-1.13	-1.04	-1.05
node 1-2	-1.61	-1.60	-1.52	-1.50
node 3-4	-1.38	-1.35	-1.30	-1.26
node 5-7	-1.15	-1.14	-1.08	-1.06
node 8-10	-0.96	-0.97	-0.92	-0.93
node 11-14	-0.91	-0.95	-0.85	-0.88
node 15-19	-0.95	-1.01	-0.85	-0.90
direction STDV	23.8	18.3	29.8	19.2
direction BIAS	-1.3	-1.4	-1.6	-1.6

Table 1: Biases and standard deviation of ERS-2 versus ECMWF FG winds in m/s for speed and degrees for direction.

observed for QuikSCAT data when restricted to an area well-covered by ERS-2 (20N-90N, 80W-20E). Figure 17 shows time series for that area for both ERS-2 (top panel) and QuikSCAT (lower panel) for the period between 1 January 2004 and 8 September 2008 (end of Cycle 139). Results are displayed for at ECMWF actively assimilated data, i.e., CMOD5/CMOD5.4 winds for ERS-2 and 4%-reduced QuikSCAT winds on a 50km resolution. The quick development of a negative bias for both ERS-2 and QuikSCAT data during the previous few Cycles is also observed for other years.

Note the increase in ERS-2 wind speed as used at ECMWF since the introduction of the new ECMWF model cycle on 7 June 2007 (Figure 17). It reflects a switch at ECMWF from the CMOD5 to CMOD5.4 model function, which has enhanced the scatterometer wind speed by 0.48 m/s.

The standard deviation of UWI wind speed versus ECMWF FG was, compared to Cycle 138, slightly higher (1.31 m/s, was 1.29 m/s).

For Cycle 139 the (UWI - FG) direction standard deviations were mostly ranging between 20 and 40 degrees (Figure 8), which represents nominal variations. Except from 6-8 September 2008, i.e., at the end of Cycle 139, the standard deviation was much enhanced. No effect was visible in the comparison between at ECMWF de-aliased CMOD4 winds and ECMWF FG winds (Figure 10). Therefore, this indicates a temporary problem in the de-aliasing algorithm of the UWI ESACA processor. As a result, average STDV for UWI wind direction was, compared to Cycle 138 higher (29.8 degrees, was 23.8 degrees). For at ECMWF de-aliased winds performance was slightly worse as well (STDV 19.2 degrees, was 18.3 degrees).

2.5 Scatterplots

Scatterplots of FG winds versus ERS-2 winds are displayed in Figures 13 to 16. Values of standard deviations and biases are slightly different from those displayed in Table 1. Reason for this is that, for plotting purposes, the in 0.5 m/s resolution ERS-2 winds have been slightly perturbed (increases scatter with 0.02 m/s), and that zero wind-speed ERS-2 winds have been excluded (decreases scatter by about 0.05 m/s).

The scatterplot of UWI wind speed versus FG (Figure 13) is very similar to that for (at ECMWF inverted) de-aliased CMOD4 winds (Figure 15). It confirms that the ESACA inversion scheme is working properly.

Winds derived on the basis of CMOD5 are displayed in Figure 16. The relative standard deviation is lower than for CMOD4 winds (1.28 m/s versus 1.33 m/s). Compared to ECMWF FG, CMOD5 winds are 0.58 m/s slower.

Figure Captions

Figure 1: Evolution of the performance of the ERS-2 scatterometer averaged over 5-weekly Cycles from 12 December 2001 (Cycle 69) to 8 September 2008 (end Cycle 139) for the UWI product (solid, star) and de-aliased winds based on CMOD4 (dashed, diamond). Results are based on data that passed the UWI QC flags. For Cycle 85 two values are plotted; the first value for a global set, the second one for a regional set (for details see the corresponding cyclic report). Dotted lines represent values for Cycle 59 (5 December 2000 to 17 January 2001), i.e. the last stable Cycle of the nominal period. From top to bottom panel are shown the normalized distance to the cone (CMOD4 only) the standard deviation of the wind speed compared to FG winds, the corresponding bias (for UWI winds the extremes in node-wise averages are shown as well), and the standard deviation of wind direction compared to FG.

Figure 2: Average number of observations per 12H and per 125km grid box (top panel) and wind climate (lower panel) for UWI winds that passed the UWI flags QC and a check on the collocated ECMWF land and sea-ice mask.

Figure 3: The same as Figure 2, but now for the relative bias (top panel) and standard deviation (lower panel) with ECMWF first-guess winds.

Figure 4: Ratio of $< \sigma_0^{0.625} > / < \mathrm{CMOD4(FirstGuess)}^{0.625} >$ converted in dB for the fore beam (solid line), mid beam (dashed line) and aft beam (dotted line), as a function of incidence angle for descending and ascending tracks. The thin lines indicate the error bars on the estimated mean. First-guess winds are based on the in time closest (+3h, +6h, +9h, or +12h) T799 forecast field, and are bilinearly interpolated in space.

Figure 5: Time series of the difference in incidence angle between the fore and aft beam. Red stars indicate the occurrences for which the combined k_p-yaw flag was set.

Figure 6: Mean normalized distance to the cone computed every 6 hours for nodes 1-2, 3-4, 5-7, 8-10, 11-14 and 15-19). The dotted curve shows the number of incoming triplets in logarithmic scale (1 corresponds to 60,000 triplets) and the dashed one indicates the fraction of complete (based on the land and sea-ice mask at ECMWF) sea-located triplets rejected by ESA flags, or by the wind inversion algorithm (0: all data kept, 1: no

data kept).

Figure 7: Mean (solid line) and standard deviation (dashed line) of the wind speed difference UWI - first guess for the data retained by the quality control.

Figure 8: Same as Fig. 7, but for the wind direction difference. Statistics are computed for winds stronger than 4 m/s.

Figures 9 and 10: Same as Fig. 7 and 8 respectively, but for the de-aliased CMOD4 data.

Figure 11: Locations of data during Cycle 139 for which UWI winds are more than 8 m/s weaker (top panel) respectively stronger (lower panel) than FG, and on which QC on UWI flags and the ECMWF land/sea-ice mask was applied.

Figure 12: Comparison between UWI winds (in red) and ECMWF FG winds (in blue) for hurricane Hanna on 3 September 2008 (top panel). The lower panel shows the usage of this data in the ECMWF analysis system. Fat, large barbs indicate (CMOD5.4-based) winds that were actively used, while thin, small barbs were not used (mostly because of data thinning). Solid and grey contours are surface-wind streamlines for the ECMWF analysis respectively ECMWF first guess.

Figure 13: Two-dimensional histogram of first guess and UWI wind speeds, for the data kept by the UWI flags, and QC based on the ECMWF land and sea-ice mask. Circles denote the mean values in the y-direction, and squares those in the x-direction.

Figure 14: Same as Fig. 13, but for wind direction. Only winds stronger than 4m/s are taken into account.

Figure 15: Same as Fig. 13, but for de-aliased CMOD4 winds.

Figure 16: Same as Fig. 13, but for de-aliased CMOD5 winds.

Figure 17: Wind-speed bias relative to FG winds for actively assimilated ERS-2 winds (based on CMOD5 before 7 June 2007; CMOD5.4 afterwards) for nodes 1-19 (top panel) respectively 50-km QuikSCAT (based on the QSCAT-1 model function and reduced by 4%) for nodes 5-34 (lower panel), averaged over the area (20N-90N, 80W-20E), and displayed for the period 1 January 2004 - 8 September 2008. Fat curves represent centred 15-day running means, thin curves values for 6-hourly periods. Vertical dashed blue lines mark ECMWF model changes.
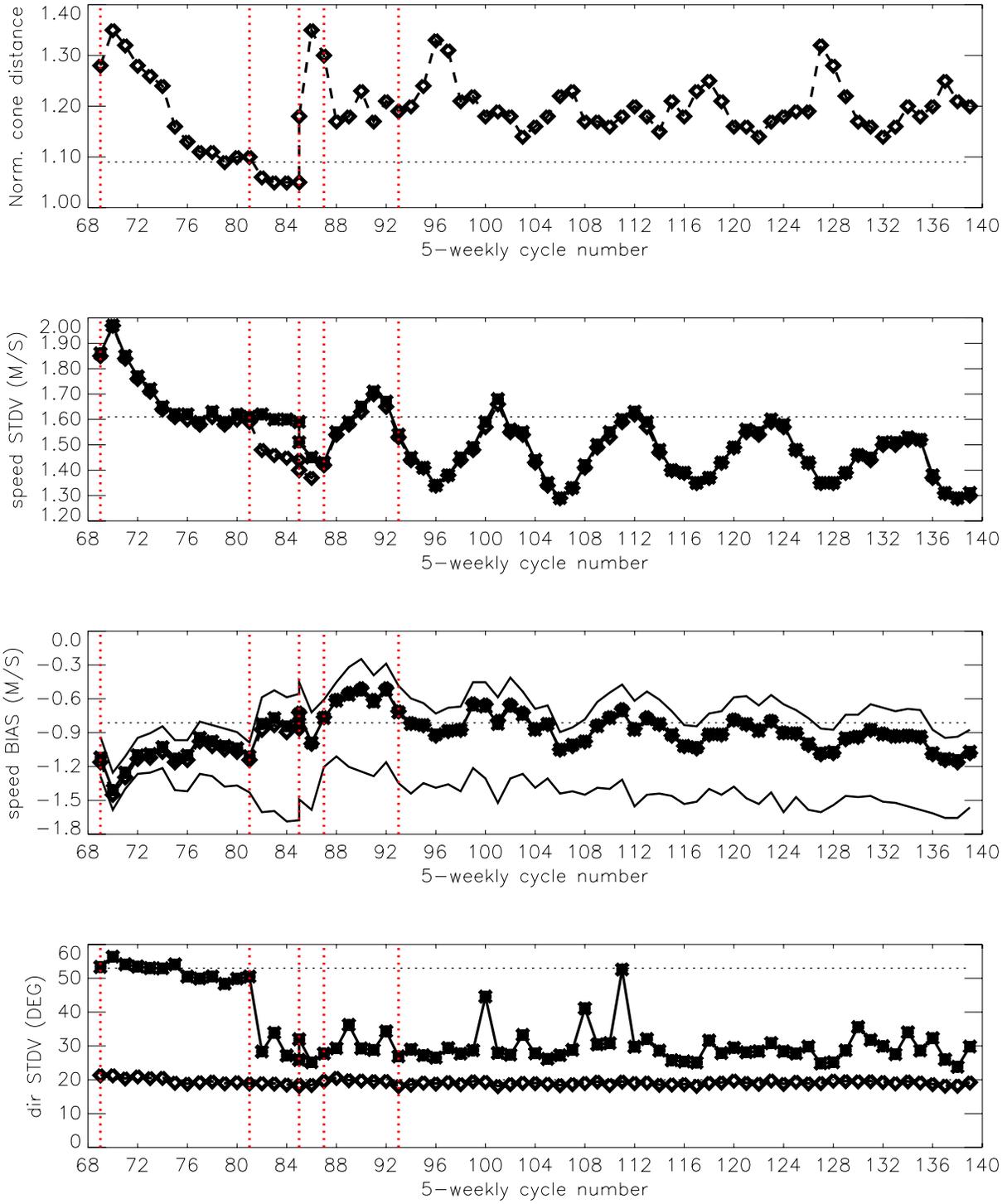
Figure 1

NOBS (ERS-2 UWI), per 12H, per 125km box
average from 2008080500 to 2008090818 GLOB:1.89
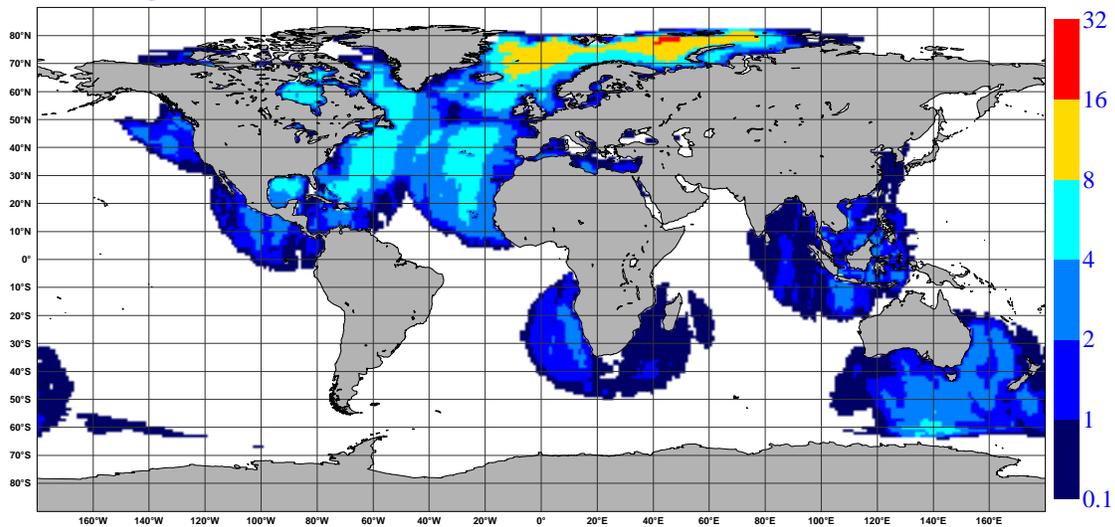
AVERAGE (ERS-2 UWI), in m/s.
average from 2008080500 to 2008090818 GLOB:6.24
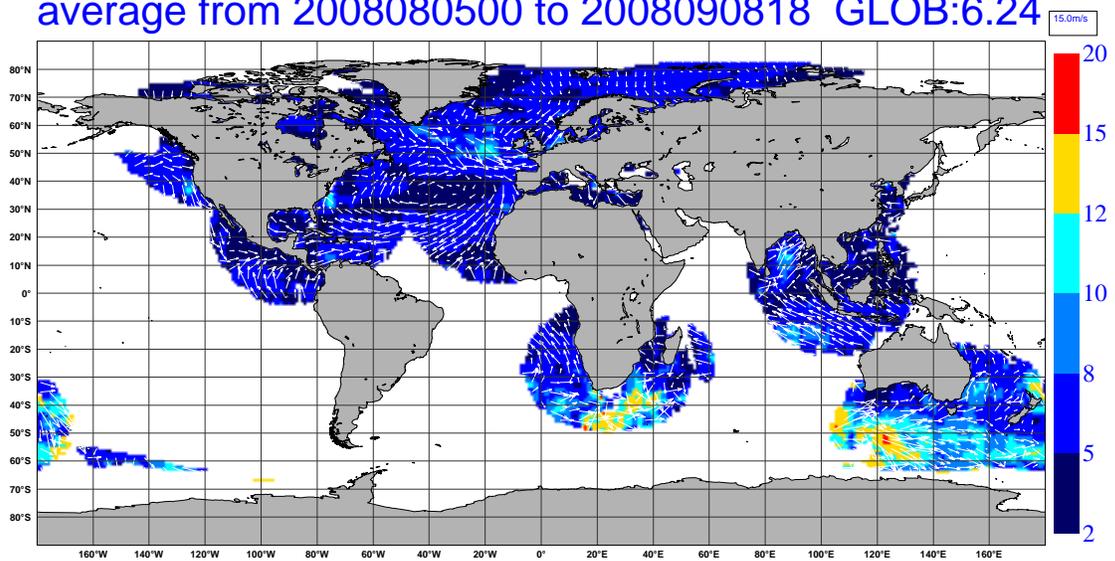
Figure 2

BIAS (ERS-2 UWI vs FIRST-GUESS), in m/s.
average from 2008080500 to 2008090818 GLOB:-1.02
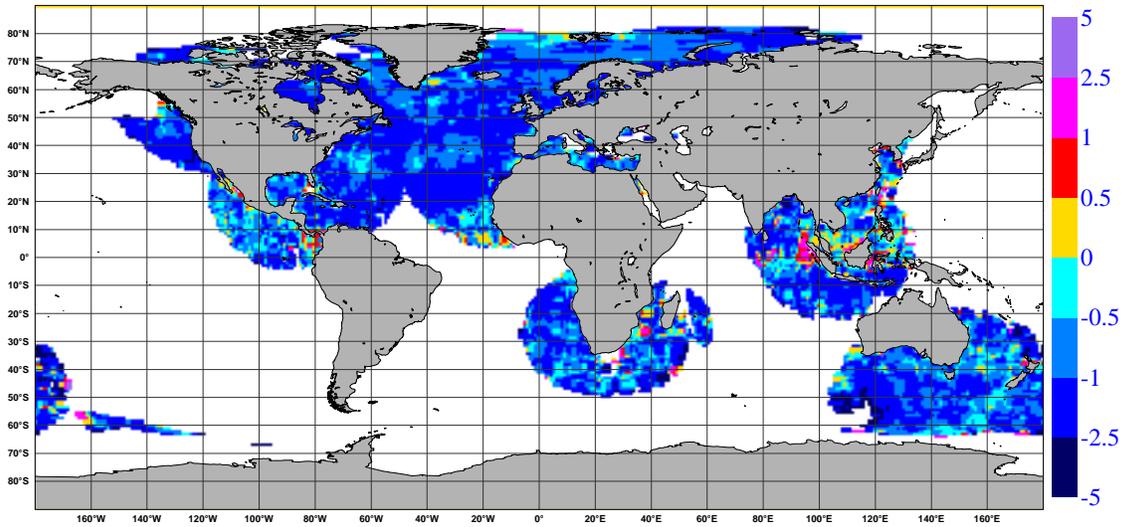
STDV (ERS-2 UWI vs FIRST-GUESS), in m/s.
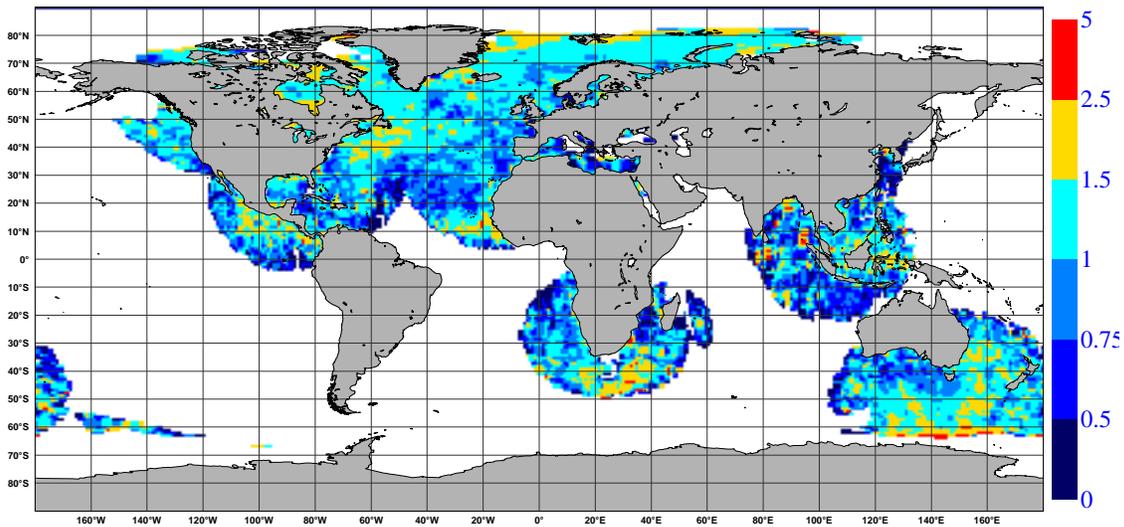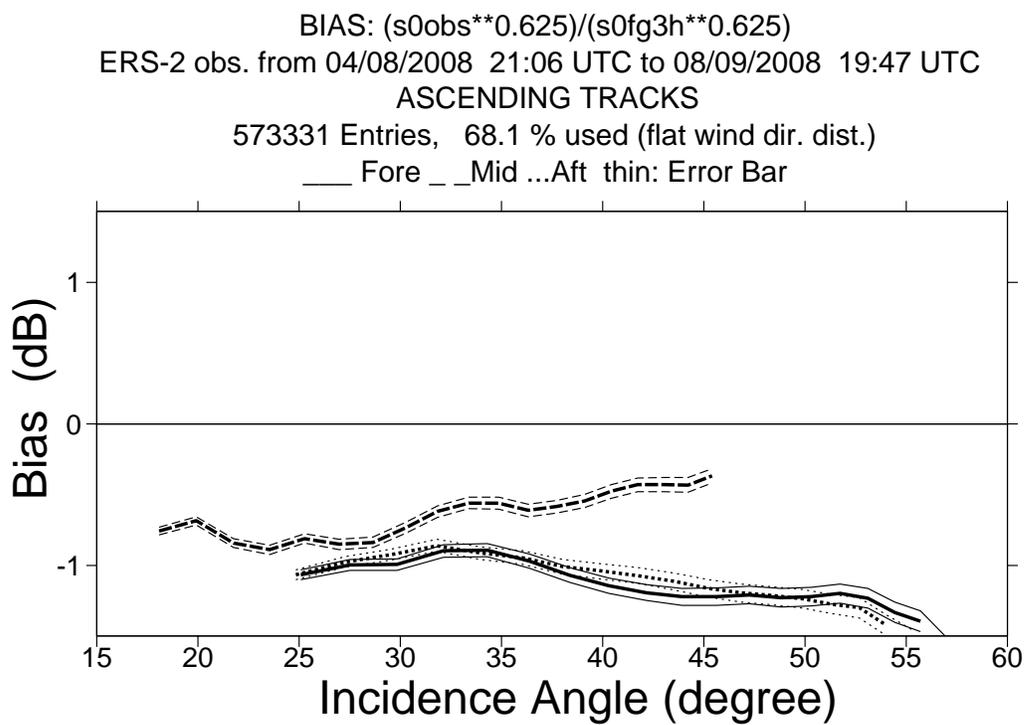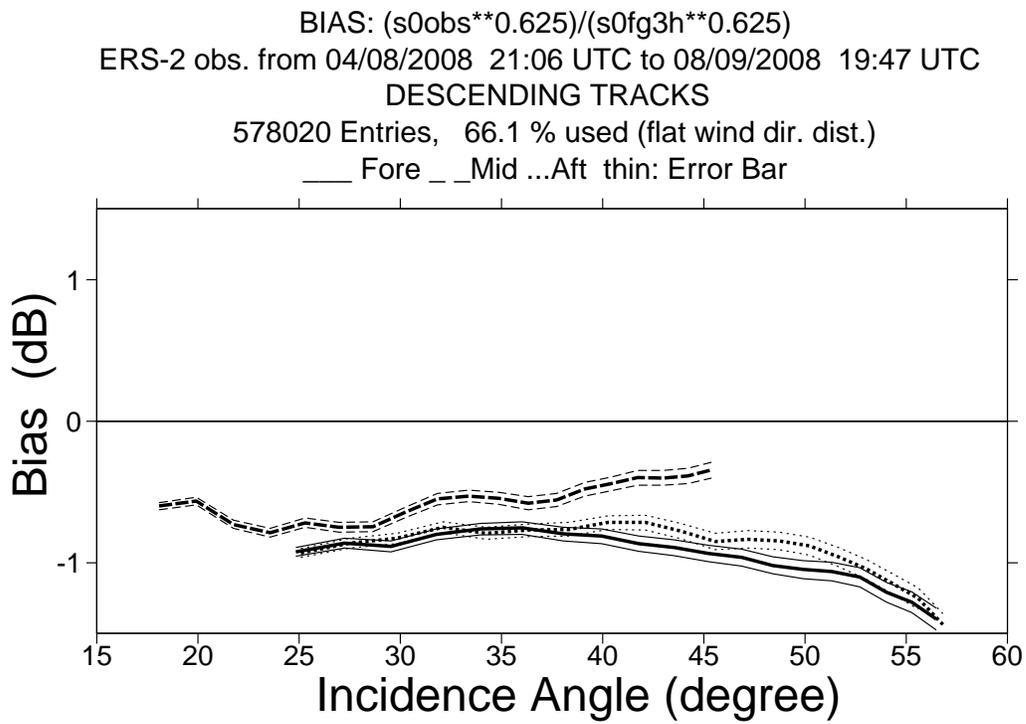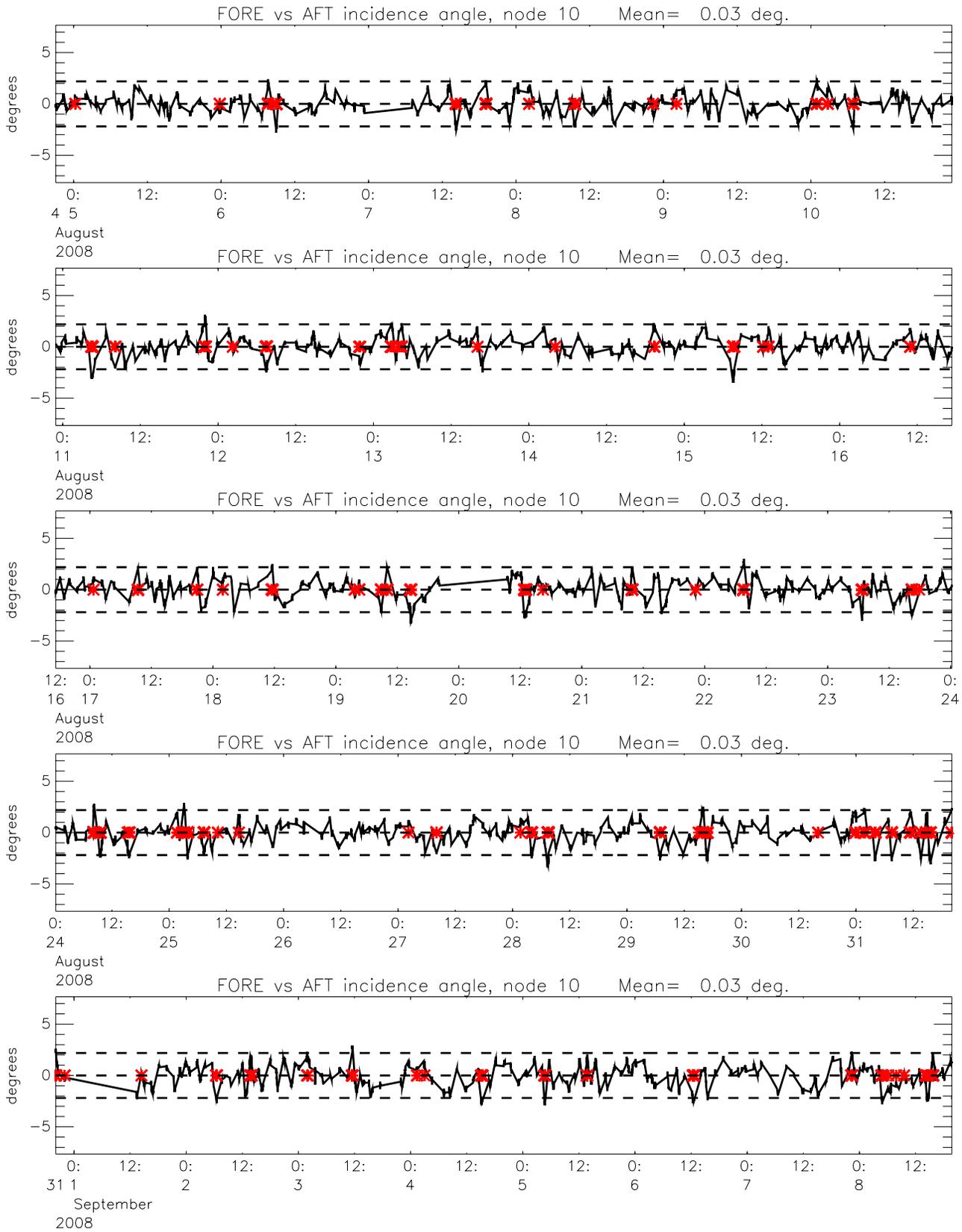average from 2008080500 to 2008090818 GLOB:1.06

Figure 3

BIAS: (s0obs**0.625)/(s0fg3h**0.625)
ERS-2 obs. from 04/08/2008 21:06 UTC to 08/09/2008 19:47 UTC
DESCENDING TRACKS
578020 Entries,   66.1 % used (flat wind dir. dist.)
___ Fore _ _Mid ...Aft thin: Error Bar

BIAS: (s0obs**0.625)/(s0fg3h**0.625)
ERS-2 obs. from 04/08/2008 21:06 UTC to 08/09/2008 19:47 UTC
ASCENDING TRACKS
573331 Entries,   68.1 % used (flat wind dir. dist.)
___ Fore _ _Mid ...Aft thin: Error Bar

Figure 4

10

Figure 5

Monitoring of Sigma0 triplets versus CMOD4 for ERS-2

from 2008080500 to 2008090818

(solid) mean normalised distance to the cone over 6 h

(dashed) fraction of complete sea-point observations rejected by ESA flag or CMOD4 inversion

(dotted) total number of data in log. scale (1 for 60000)
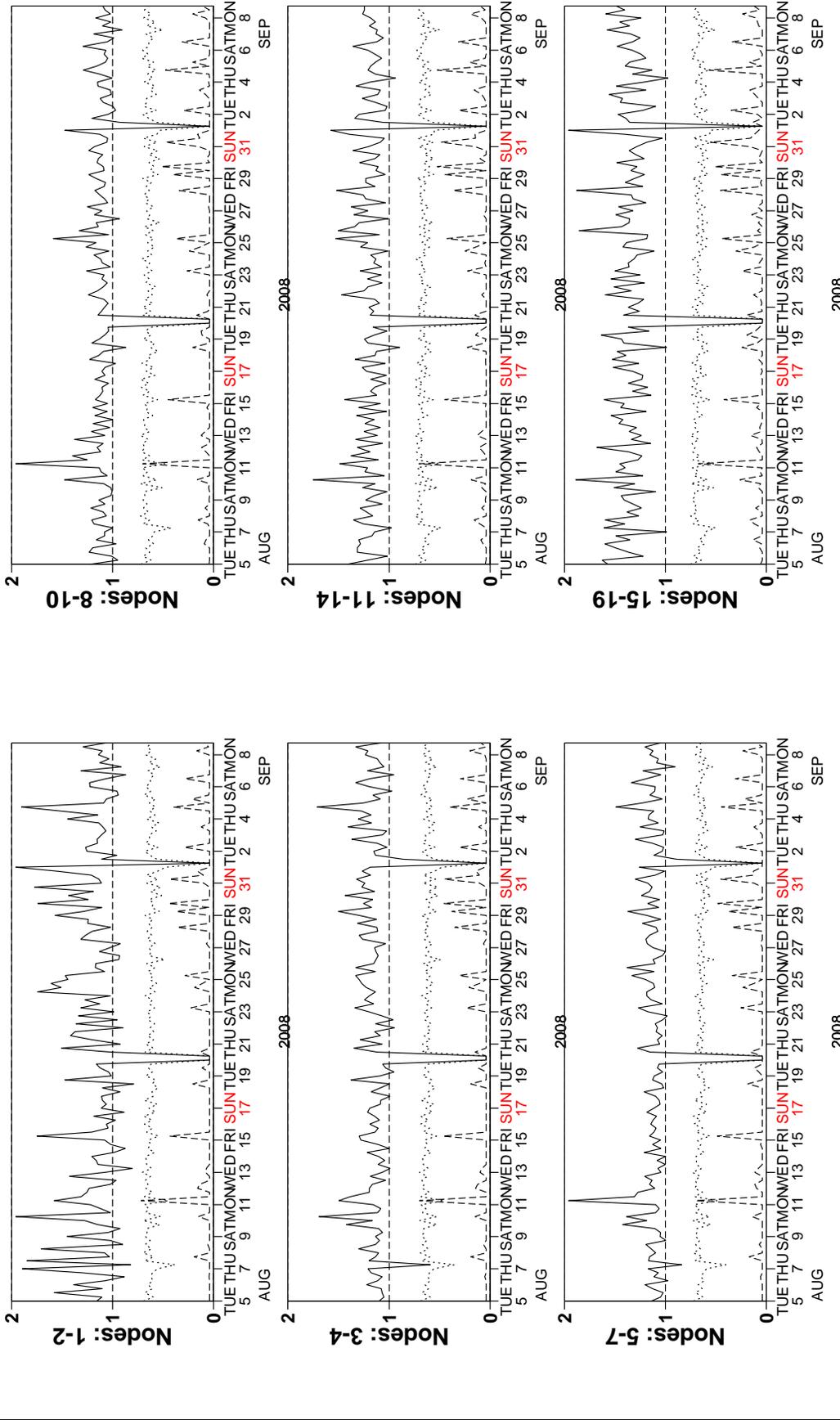
Figure 6

Figure 7

Monitoring of UWI winds versus First Guess for ERS-2

from 2008080500 to 2008090818

(solid) wind direction bias UWI - First Guess over 6h (deg.)

(dashed) wind direction standard deviation UWI - First Guess over 6h (deg.)
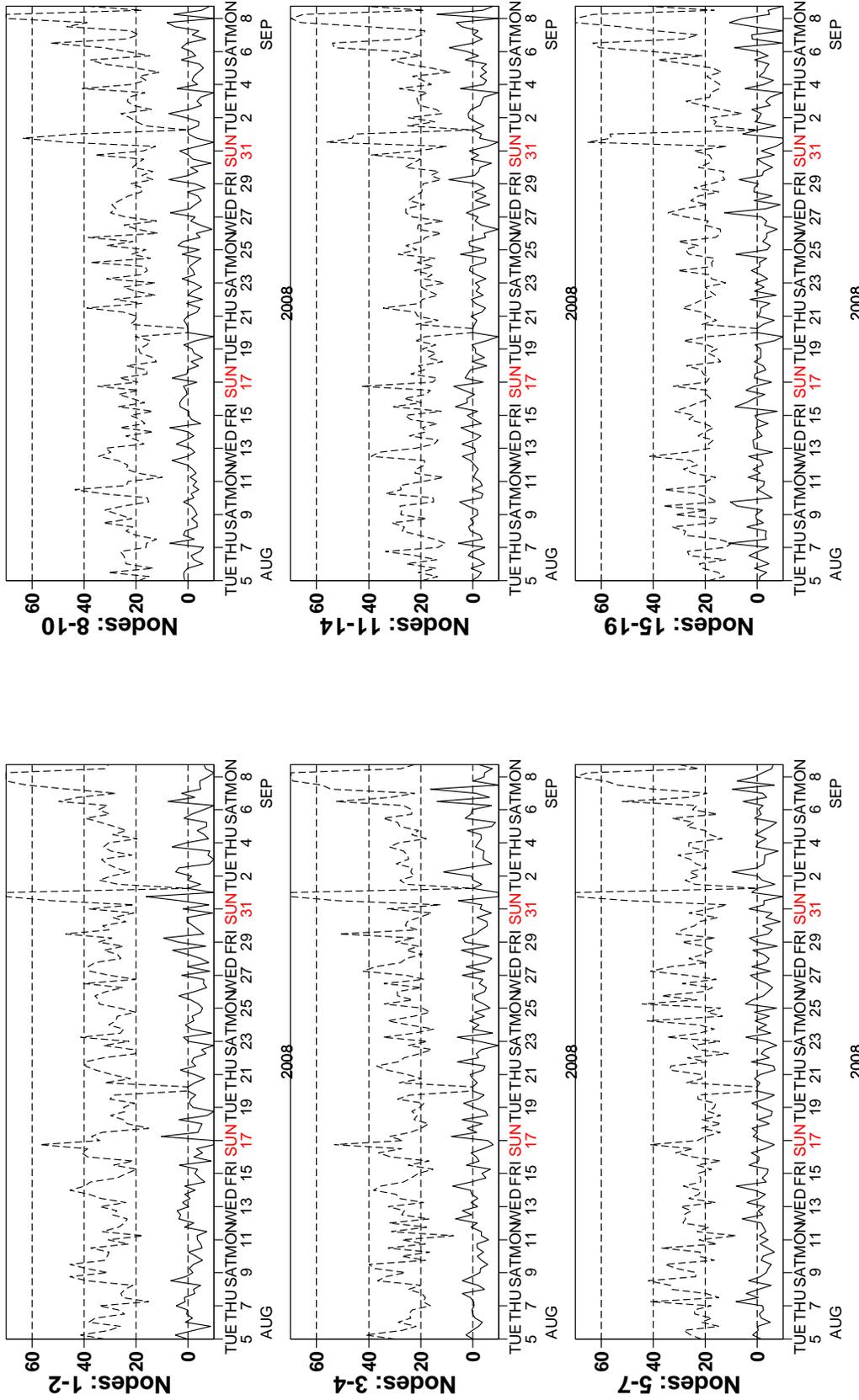
Figure 8

Monitoring of de-aliased CMOD4 winds versus First Guess for ERS-2

from 2008080500 to 2008090818

(solid) wind speed bias CMOD4 - First Guess over 6h (deg.)

(dashed) wind speed standard deviation CMOD4 - First Guess over 6h (deg.)

Figure 9

15

Figure 10

16
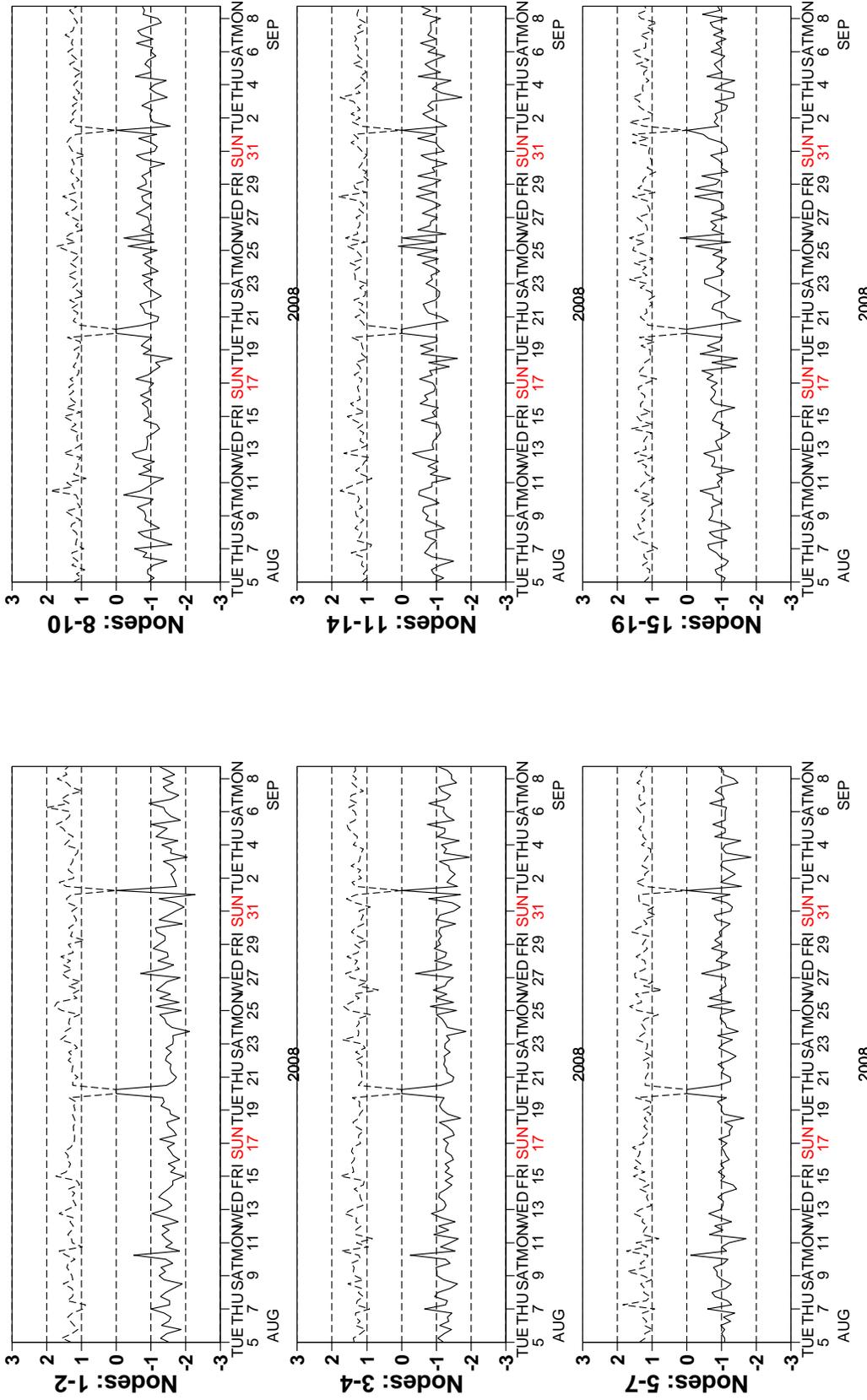
UWI winds more than 8 m/s stronger than ECMWF First Guess
CYCLE 139, 2008080500 to 2008090818, QC on ESA flags
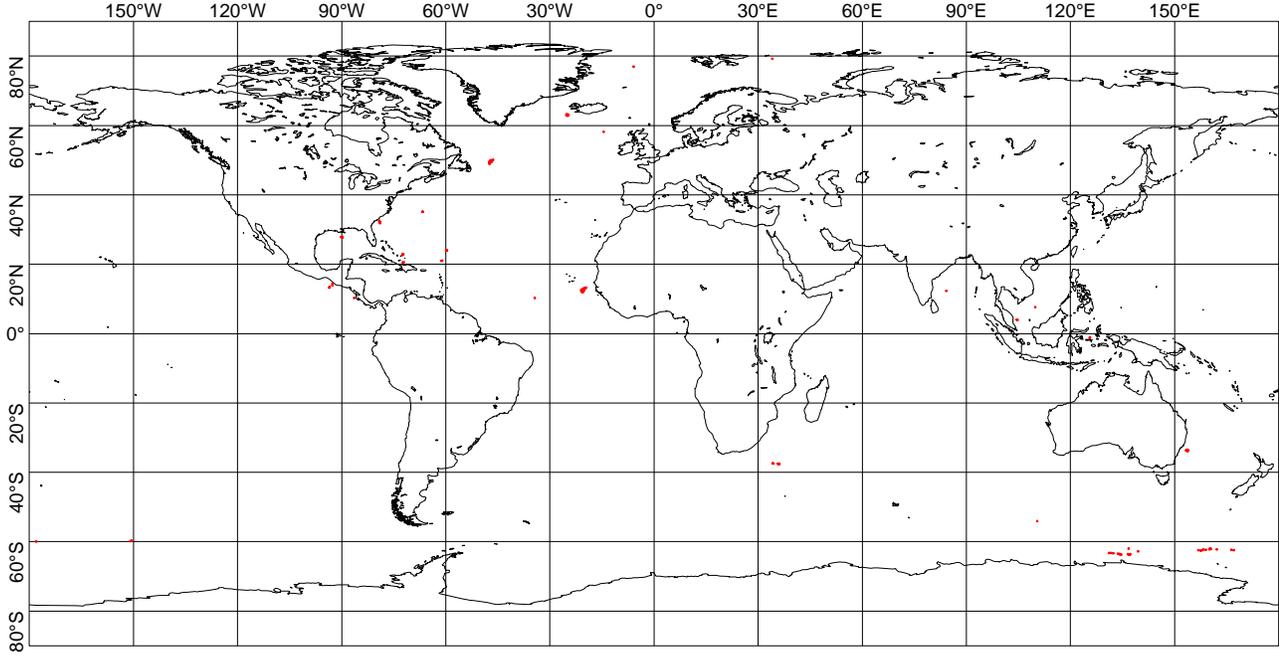
Figure 11

UWI winds (red) versus ECMWF FG winds (blue)
Tropical storm Hanna 20080903 03:24 UTC
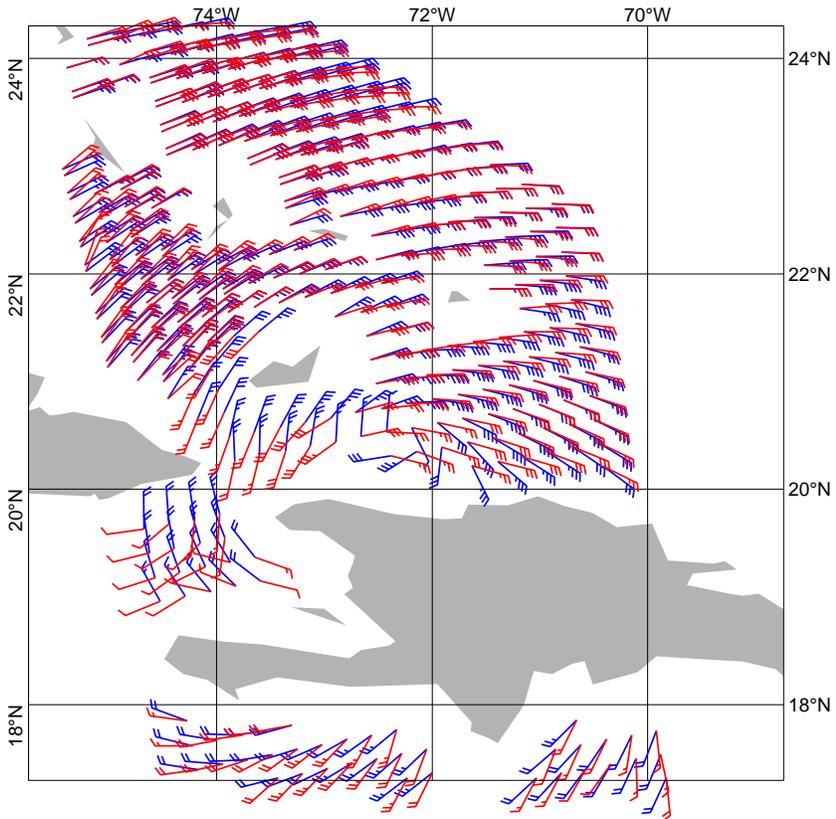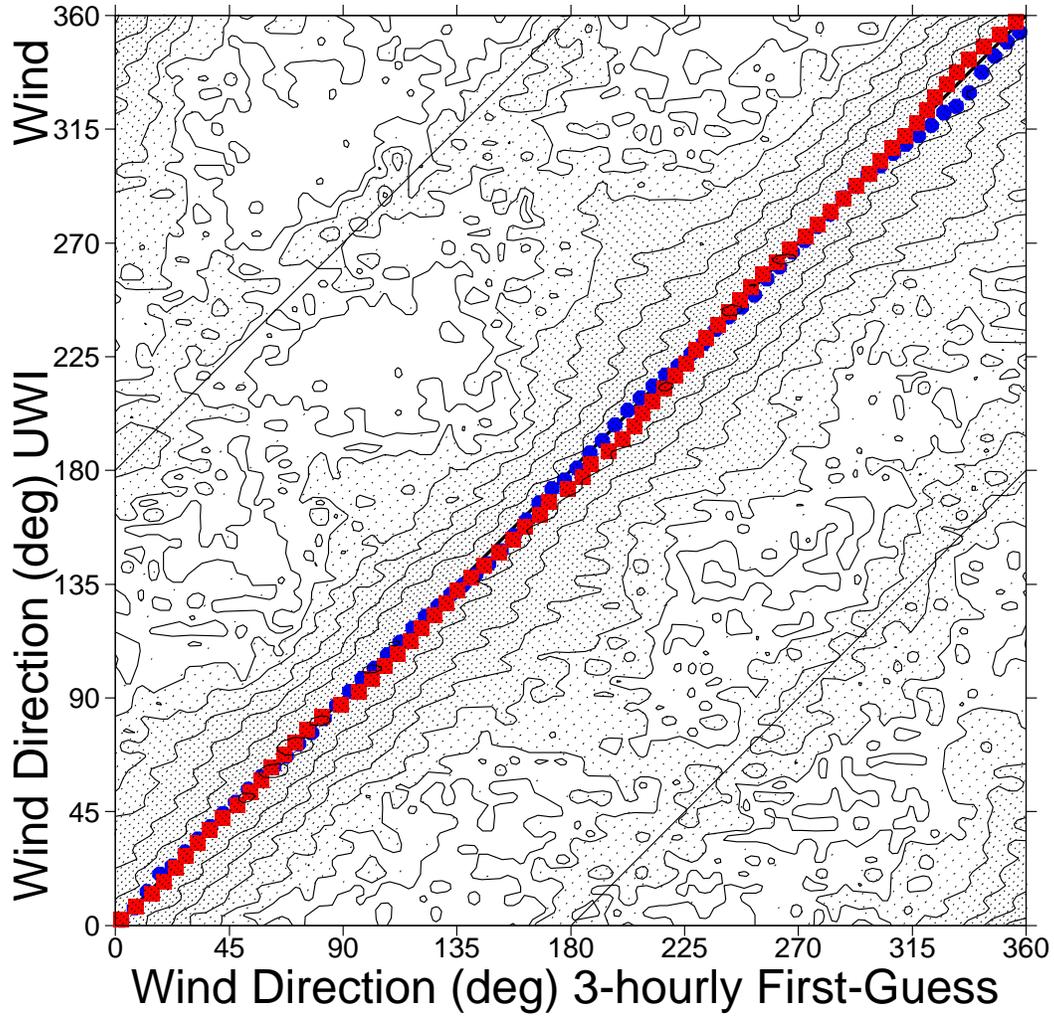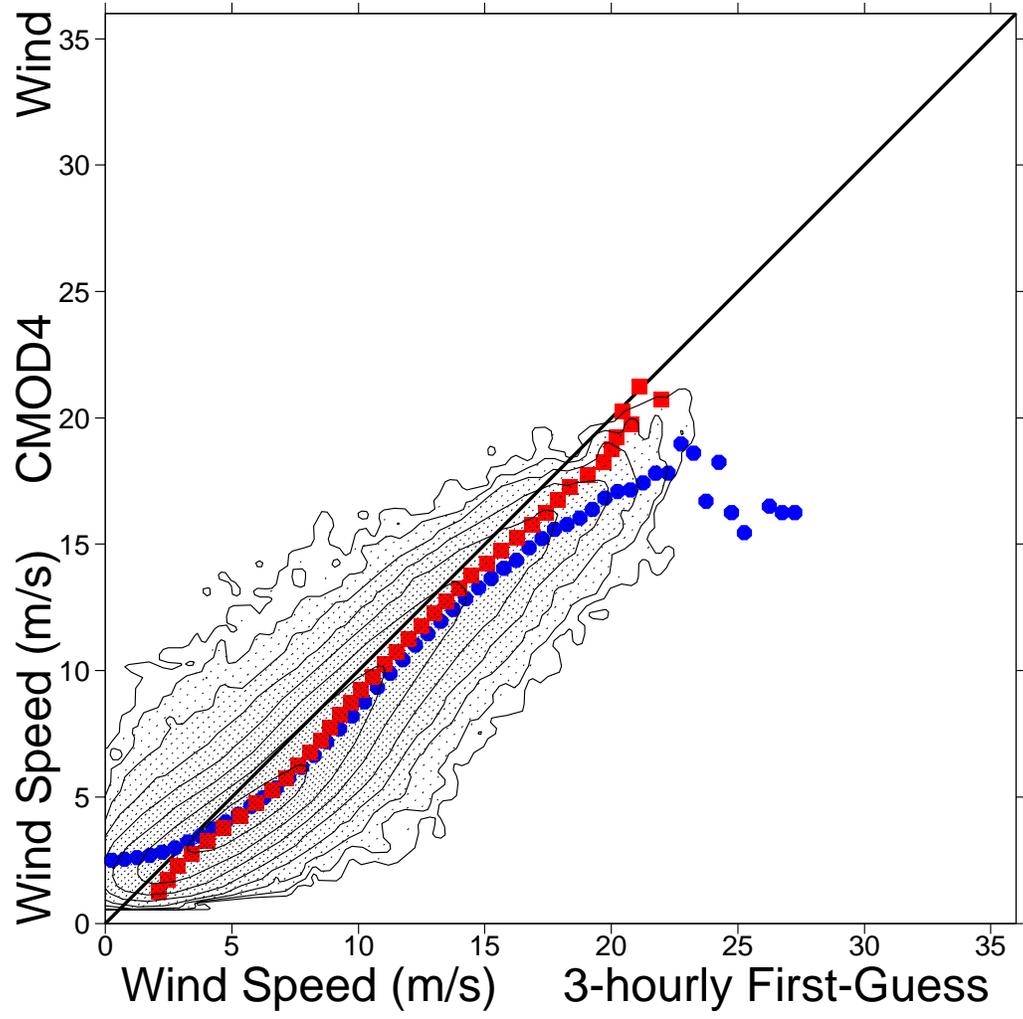
Scatterometer winds for 2008090306
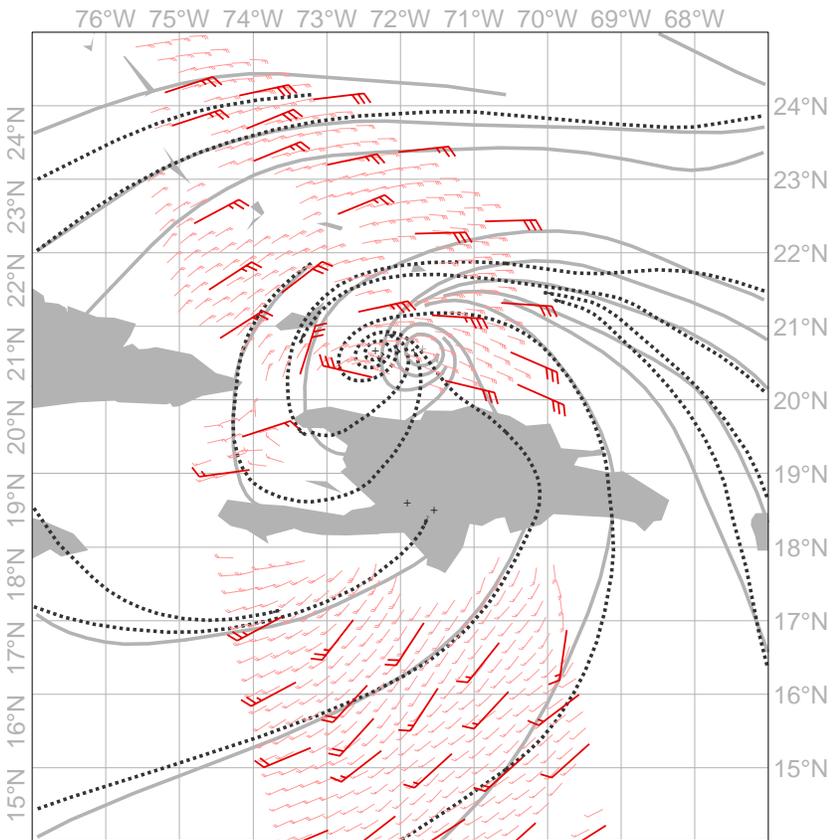
Figure 12

ECMWF 3-hourly First-Guess winds versus UWI winds
from 2008080500 to 2008090818
=   1151351, db contour levels, 5 db step, 1st level at   5.6 db
m(y-x)= -1.04 sd(y-x)= 1.33 sdx= 3.31 sdy= 3.02 pcxy= 0.957

Figure 13

19
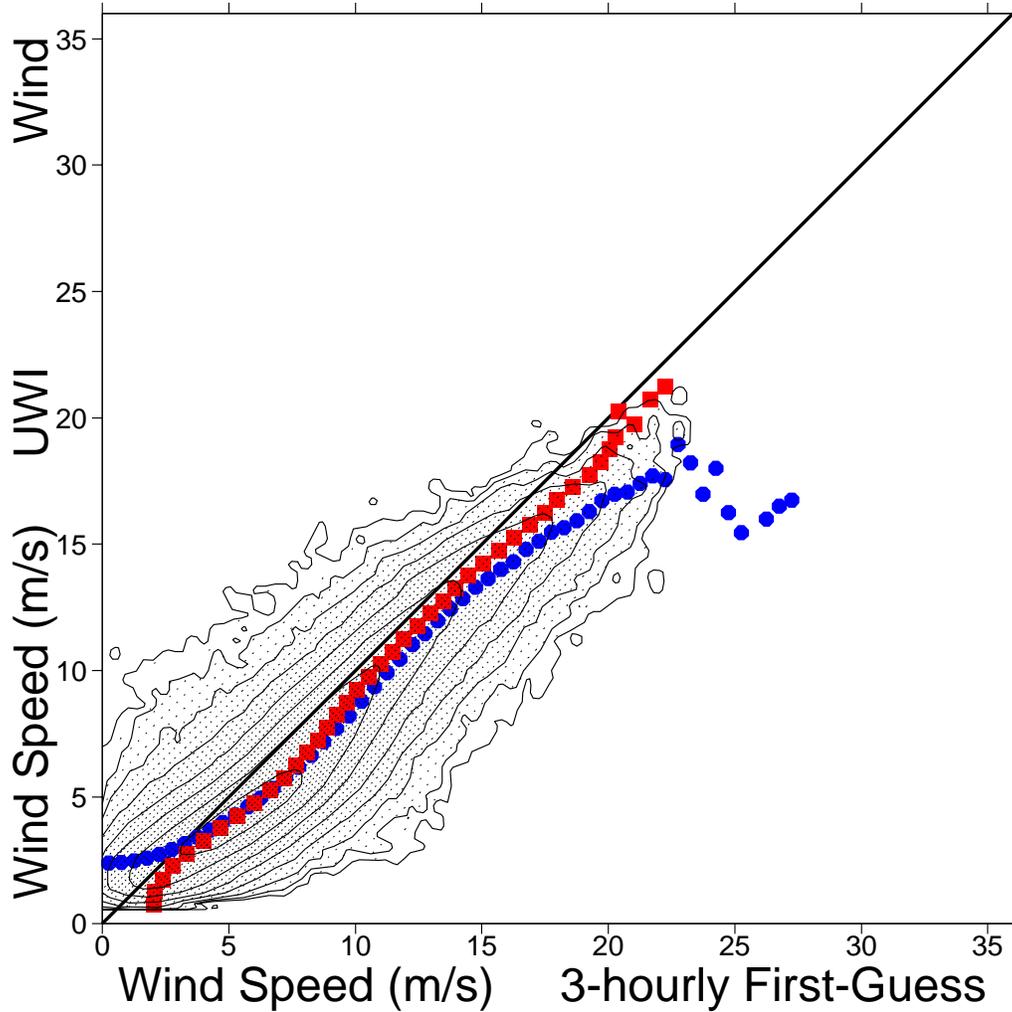
ECMWF 3-hourly First-Guess winds versus UWI winds
from 2008080500 to 2008090818
= 855152 (|f| gt 4.00 m/s), db contour levels, 5 db step, 1st level at 4.3 db
m(y-x)= -1.85 sd(y-x)= 29.80 sdx=102.29 sdy=102.61 pcxy= 0.979

Figure 14

ECMWF 3-hourly First-Guess winds versus CMOD4 winds
from 2008080500 to 2008090818
= 1131784, db contour levels, 5 db step, 1st level at 5.5 db
m(y-x)= -1.05 sd(y-x)= 1.33 sdx= 3.28 sdy= 3.00 pcxy= 0.956

Figure 15

ECMWF 3-hourly First-Guess winds versus CMOD5 winds
from 2008080500 to 2008090818
= 1109301, db contour levels, 5 db step, 1st level at 5.5 db
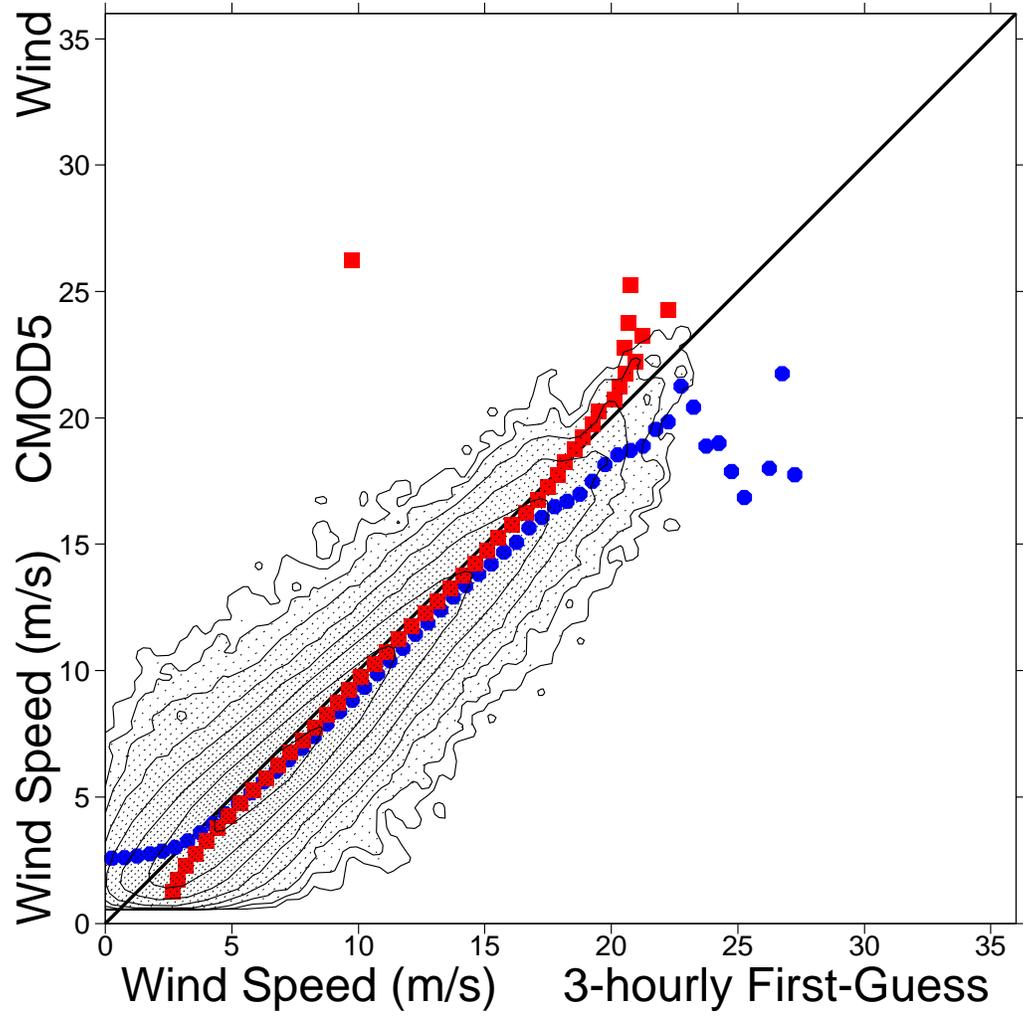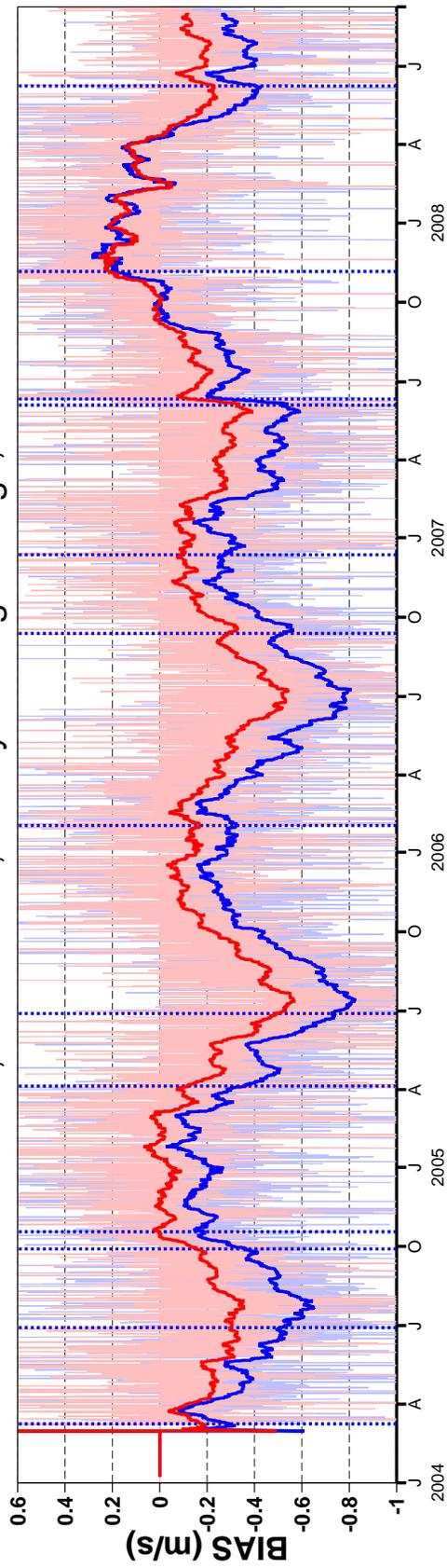m(y-x)= -0.58 sd(y-x)= 1.28 sdx= 3.24 sdy= 3.13 pcxy= 0.959

Figure 16

Figure 17